



HAL
open science

A spatio-temporal model to describe the spread of within a laying flock

Pascal Zongo, Anne-France Viet, Pierre Magal, Catherine Beaumont

► **To cite this version:**

Pascal Zongo, Anne-France Viet, Pierre Magal, Catherine Beaumont. A spatio-temporal model to describe the spread of within a laying flock. *Journal of Theoretical Biology*, 2010, 267 (4), pp.595. 10.1016/j.jtbi.2010.09.030 . hal-00637816

HAL Id: hal-00637816

<https://hal.science/hal-00637816>

Submitted on 3 Nov 2011

HAL is a multi-disciplinary open access archive for the deposit and dissemination of scientific research documents, whether they are published or not. The documents may come from teaching and research institutions in France or abroad, or from public or private research centers.

L'archive ouverte pluridisciplinaire **HAL**, est destinée au dépôt et à la diffusion de documents scientifiques de niveau recherche, publiés ou non, émanant des établissements d'enseignement et de recherche français ou étrangers, des laboratoires publics ou privés.

Author's Accepted Manuscript

A spatio-temporal model to describe the spread of *Salmonella* within a laying flock

Pascal Zongo, Anne-France Viet, Pierre Magal, Catherine Beaumont

PII: S0022-5193(10)00504-7
DOI: doi:10.1016/j.jtbi.2010.09.030
Reference: YJTBI6170



www.elsevier.com/locate/jtbi

To appear in: *Journal of Theoretical Biology*

Received date: 1 April 2010
Revised date: 21 September 2010
Accepted date: 21 September 2010

Cite this article as: Pascal Zongo, Anne-France Viet, Pierre Magal and Catherine Beaumont, A spatio-temporal model to describe the spread of *Salmonella* within a laying flock, *Journal of Theoretical Biology*, doi:[10.1016/j.jtbi.2010.09.030](https://doi.org/10.1016/j.jtbi.2010.09.030)

This is a PDF file of an unedited manuscript that has been accepted for publication. As a service to our customers we are providing this early version of the manuscript. The manuscript will undergo copyediting, typesetting, and review of the resulting galley proof before it is published in its final citable form. Please note that during the production process errors may be discovered which could affect the content, and all legal disclaimers that apply to the journal pertain.

1 A spatio-temporal model to describe the spread of
2 *Salmonella* within a laying flock

3 Pascal Zongo^{a,1}, Anne-France Viet^{b,c}, Pierre Magal^d, Catherine Beaumont^a

4 ^aINRA, UR 083 Recherches Avicoles, 37380 Nouzilly, France.

5 ^bINRA, UMR1300 Bio-agression Epidémiologie et Analyse de Risques, 44307 Nantes, France.

6 ^cONIRIS, UMR1300 Bio-agression Epidémiologie et Analyse de Risques, 44307 Nantes, France.

7 ^dUMR CNRS 5251 IBM-INRIA sud-ouest Anubis, Université Victor Segalen Bordeaux2, 33000
8 Bordeaux, France.

9 **Abstract**

10 *Salmonella* is one of the major sources of toxi-infection in humans, most often
11 because of consumption of poultry products. The main reason for this association is
12 the presence in hen flocks of silent carriers, i.e. animals harbouring *Salmonella* with-
13 out expressing any visible symptoms. Many prophylactic means have been developed
14 to reduce the prevalence of *Salmonella* carrier-state. While none allows a total re-
15 duction of the risk, synergy could result in a drastic reduction of it. Evaluating the
16 risk by modeling would be very useful to estimate such gain in food safety. Here,
17 we propose an individual-based model which describes the spatio-temporal spread
18 of *Salmonella* within a laying flock and takes into account the host response to bac-
19 terial infection. The model includes the individual bacterial load and the animals'
20 ability to reduce it thanks to the immune response, i.e. maximum bacterial dose
21 that the animals may resist without long term carriage and, when carriers, length of
22 bacterial clearance. For model validation, we simulated the *Salmonella* spread under
23 published experimental conditions. There was a good agreement between simulated
24 and observed published data. This model will thus allow studying the effects, on the
25 spatiotemporal distribution of the bacteria, of both mean and variability of different
26 elements of host response.

27 *Keywords:*

28 *Salmonella*; Individual-based model; bacterial transmission; individual
29 heterogeneity

¹Corresponding author
Pascal.Zongo@tours.inra.fr (Pascal Zongo)

30 1. Introduction

31 *Salmonella* is a major cause of human toxi-infection and poultry products, eggs
32 and egg products, are the most common source of human *salmonellosis*. *Salmonella*
33 enterica serovar Enteritidis is the strain most often associated with salmonellosis
34 caused by poultry products (EFSA, 2009; Humphrey, 1990). *Salmonella* enteritidis
35 can colonize the gastrointestinal tract of fowls as well as their systemic organs, such as
36 spleen or liver, for long periods. This colonization does not cause clinical signs. This
37 silent carrier-state will in turn lead to between animals transmission. Horizontal
38 transmission within the flock may occur either directly from one infected animal
39 to another fowl, especially in the same cage, through aerosols (Gast et al., 2002;
40 Lever and Williams, 1996) or indirectly because of environmental contamination,
41 mainly through water and feed, as observed in Nakamura et al., 1994. Vertical
42 transmission though trans-ovarian route may also occur (Humphrey and Lanning,
43 1988). Moreover, once the animal is infected, there is an individual variation in the
44 duration and level of bacteria excretion (Beaumont et al., 2003; Ishola, 2009).

45 Because of the importance for food safety of poultry contamination by *Salmonella*,
46 prevention of animal infection is an important research area. Many experiments have
47 been conducted to evaluate control methods to prevent animal colonization: vaccina-
48 tion (Barrow, 2007; Zhang-Barber et al., 1999), competitive exclusion (Rantala and
49 Nurmi, 1973), acidification of food, selection for increased animal genetic resistance
50 (Beaumont et al., 2009).

51 While none of these control measures results in a zero risk, their relative efficacy
52 and possibility of synergy still remains to be estimated. This may be investigated
53 through modeling of bacteria spread within a hen house including horizontal and
54 vertical transmission and animals heterogeneity once infected (level and duration of
55 excretion).

56 Models have already been proposed to study *Salmonella* spread within various
57 animal species: hens (Leslie, 1996; Prévost et al., 2006; Thomas et al., 2009), pigs
58 (Hill et al., 2008; Lurette et al., 2008) and dairy herds (Xiao et al., 2005, 2006, 2007;
59 Lanzas et al., 2008). But no model considered, at least until now, both the bacterial
60 transmission and heterogeneity of hens's response to infection. Individual variability
61 of the immune response may be introduced into stochastic individual-based models.
62 Such model patterns are largely used in ecology (Grimm et al., 2006) and were
63 already used to model the growth and migration of *Salmonella* enteritidis in hens'
64 eggs (Grijnspeerdt et al., 2005).

65 The objective of this paper is to present a stochastic individual-based model for
66 the spread of *Salmonella* within a hen house. It allows us to consider individual
67 levels of bacterial infection as well as variability of the host response, i.e. maximal

68 dose an animal may eliminate without long term infection as well as duration of
 69 bacterial clearance. The paper is organized as follows: in Section 2 we describe
 70 our individual-based model; validation and exploration of the model behaviour are
 71 presented in section 3; they are followed by a discussion and a conclusion in section
 72 4 and 5 respectively.

73 2. Model

74 The model description hereafter follows the ODD (Overview, Design concepts,
 75 Details) protocol for describing individual and agent-based models (Grimm et al.,
 76 2006).

77 2.1. Purpose

78 An individual-based model was used to represent the spatial spread of *Salmonella*
 79 within a flock of laying hens reared in cages. We assumed that all animals in a cage
 80 are infected at the same time (through contaminated food, water, rodents...) so that
 81 the individual unit of interest here is a cage. In this model, the risk of long term
 82 infection is dependant on both individual bacterial load and a stochastic threshold,
 83 corresponding to individuals' capacities of resistance to infection. When the latter
 84 are overwhelmed, persistent infection occurs. Its length and duration of immune
 85 protection after recovery are stochastic.

86 2.2. Entities, state variables, and scales

87 In this model, individuals are cages harboring hens (all of them harbor the same
 88 number of hens). Individuals are aligned in rows and each group of two rows are
 89 separated from each other by an interval allowing the farmer to take care of animals.
 90 As we are interested in the transmission via the environment, the flock is divided
 91 in grid cells, allowing us to describe the contamination in each location of the hen
 92 house. Each individual is then identified in the hen house by its position $x = (x_1, x_2)$
 93 (i.e x_1 -abscissa and x_2 -ordinate).

94 An individual is characterized by its bacterial load denoted by $B(t_n, x)$ and its
 95 health status denoted by $\mathcal{H}(t_n, x)$ at time t_n and position x . In our model, we assume
 96 that there exists an individual bacterial threshold within an individual denoted by
 97 $D(x)$ so that the individual bacterial load decreases over the time when the initial
 98 bacterial load is lower than $D(x)$, increases when the initial bacterial load is higher
 99 than $D(x)$ and remains constant when it is equal to $D(x)$ (see Figure 2(a)). An
 100 individual infection beyond the threshold results in systemic infection (because of
 101 overwhelming of individuals capacities to reduce bacterial load).

Table 1: State variables given for each location $x = (x_1, x_2)$ in the hen house at a time t_n .

$C(t_n, x)$	Density of bacterial environmental infection
$B(t_n, x)$	Level of bacterial load within an individual
$\mathcal{H}(t_n, x)$	Health status of the individual
$D(x)$	Bacterial threshold within the individual

102 At the same time t_n and position x , the level of contamination in environment
 103 is represented by $C(t_n, x)$. Note that, for positions that do not contain individuals,
 104 variables $B(t_n, x)$, $\mathcal{H}(t_n, x)$ and $D(x)$ are not defined while $C(t_n, x)$ is defined.

105 The full set of variables for the individual-based model are described in Table 1.
 106 Time step for the model is one day.

107 2.3. Process overview and scheduling

108 The flowchart in Figure 1 outlines the events occurring during each time step for
 109 one given replication. Details are given by submodels in section 2.7.

110 2.4. Design concepts

111 **Interaction:** we consider interaction between one individual and those located in
 112 the neighborhood through inhalation or ingestion of bacteria excreted in the
 113 environment.

114 **Stochasticity:** two components are stochastic: threshold for bacterial load and time
 115 interval before change to next health status.

116 **Observation:** the model outputs are the health status of each individual and the
 117 density of bacteria in environment at each time step for all positions. From
 118 these outputs, we compute the percentage of individuals over time in the house
 119 and over row for each health status which are determinant for practical issues
 120 and for comparison to experimental data.

121 2.5. Initialization

122 Initialization consists in defining the size of the house, the number of rows of
 123 individuals, the number of individuals by rows and following state variables for each
 124 location. Health status ($\mathcal{H}(t_n, x)$), bacterial load ($B(t_n, x)$) and density of bacteria
 125 in the environment ($C(t_n, x)$) are initialized by the user. The threshold $D(x)$ is
 126 initialized stochastically for each replication and each individual and kept constant
 127 during the whole replication.

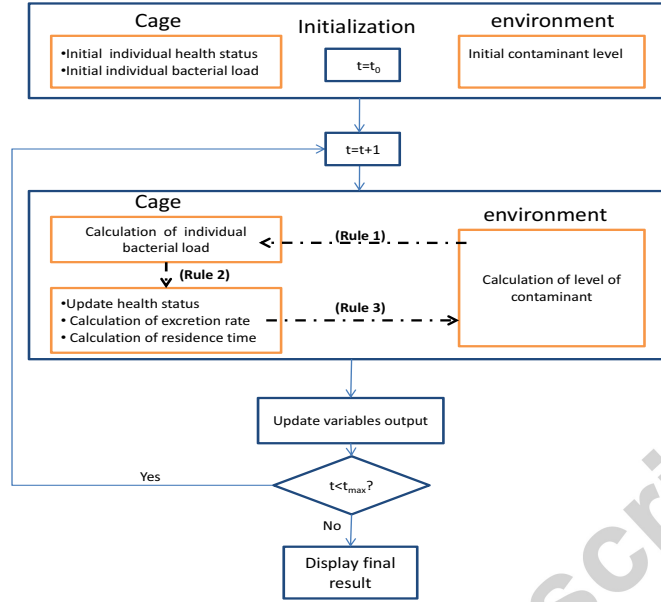


Figure 1: Flowchart showing a time step iteration. For each time step, **Rule 1** considers individual infection (ingestion or inhalation in environment) to update individual bacterial load (as described in Section 2.7.1), **Rule 2** considers the bacterial load to update health status (as described in Section 2.7.2), **Rule 3** computes the number of excreted bacteria to update the contamination level in environment (as described in Section 2.7.3).

128 2.6. Input for time varying process

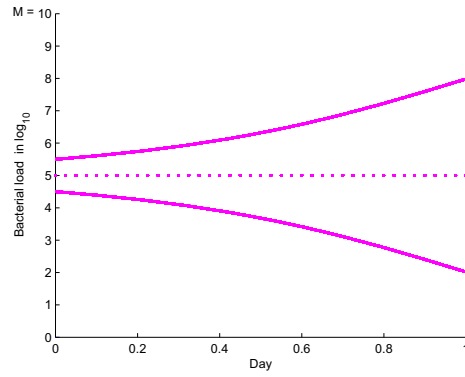
129 The model does not use input data to represent time-varying process.

130 2.7. Submodels

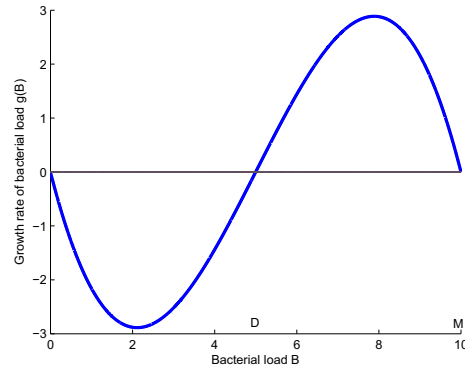
131 Further notations are needed to describe the submodels: the time interval $(0, T_{max})$
 132 is partitioned into subintervals (t_n, t_{n+1}) , with a time step $\delta t = t_{n+1} - t_n = 1$ day.

133 Let $\Omega \subset \mathbb{R}^2$ be the area covered by the hen house and denote by $x = (x_1, x_2) \in \Omega$
 134 a point of hen house. Assume that $x_1 \in (0, L_1)$ and $x_2 \in (0, L_2)$ where L_1 and L_2
 135 is the length and width of hen house respectively. We use a uniform Cartesian grid
 136 consisting of grid points (x_{1i}, x_{2j}) to partition the x_1 -component and x_2 -component
 137 interval of x where $x_{1i} = i\delta x_1$ and $x_{2j} = j\delta x_2$, $i = 0, 1, 2, \dots, N_1$, $j = 0, 1, 2, \dots, N_2$
 138 and we simplify the writing of the point (x_{1i}, x_{2j}) by $x_{i,j}$.

139 From now, an individual will be identified by the coordinates of its center $x_{a,b}$
 140 where a and b are chosen from $\{0, 1, 2, \dots, N_1\}$ and $\{0, 1, 2, \dots, N_2\}$ respectively.



(a)



(b)

Figure 2: (a) Example of evolution of Bacterial load, $B(\tau, \cdot)$ on one day, $\tau \in (t_n, t_{n+1})$. Curves with three different initial sizes of dose: $B(t_n, \cdot) = 4.5 \log_{10}$ (the bottom solid line), $B(t_n, \cdot) = 5 \log_{10} = D(\cdot)$ (the dotted line) and $B(t_n, \cdot) = 5.5 \log_{10}$ (the upper solid line). (b) Growth rate of bacterial load $g(B)$. Here, individual threshold, $D = D(\cdot)$ is set at $5 \log_{10}$, carrying capacity, M at $10 \log_{10}$ and the density of bacteria that an individual acquires by ingestion or inhalation at zero.

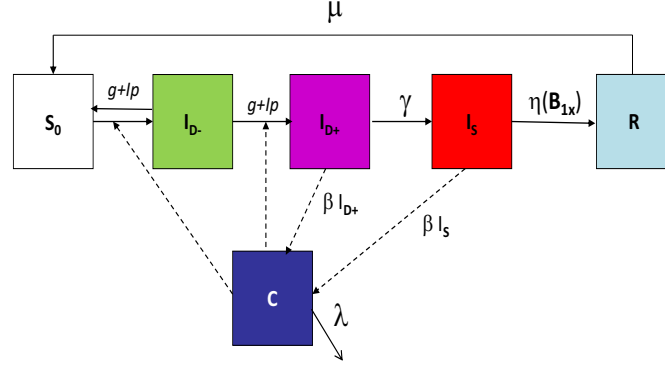


Figure 3: Evolution of health status for an individual and its interaction with the contaminant in environment at time t_n and position $x_{a,b}$: S_0 (susceptible) I_{D-} , (infected with a digestible low dose of infection), I_{D+} , (suffering from a long term digestive infection), I_S (systemic infection) and R (recovered). The force of infection $g + I_p$ is defined in Section 2.7.2. The parameters $\gamma, \eta(B_{1x}), \mu, \beta_{I_{D+}}, \beta_{I_S}$ and λ are described in Table 2.

141 2.7.1. Model for individual bacterial load within each day

142 An individual must initially be exposed to a sufficient density of bacteria to
 143 become infected (Humphrey et al., 1991; Gast, 1993; Lever and Williams, 1996). At
 144 very low dose of infection, the bacterial load within an individual will decrease over
 145 time due to the ability of the organism to overcome this infection. At the opposite,
 146 it will multiply over time when this initial dose of infection exceeds a threshold until
 147 saturation value due to the limitation of resources. We denote by M , the carrying
 148 capacity of bacterial load within an individual (i.e. maximal number of bacteria that
 149 an individual may carry) and $D(x_{a,b})$ ($0 < D(x_{a,b}) < M$), the threshold of bacteria
 150 load for which an individual at position $x_{a,b}$ is able to overcome an infection and
 151 reduce the number of bacteria over the time. We use the *strong allee effet* (Jiang
 152 and Shi, 2009; Wang and Kot, 2001) to model the growth of bacteria within an
 153 individual in the following way. Let $B(\tau, x_{a,b})$, $f(B(\tau, x_{a,b}))$ and $g(B(\tau, x_{a,b}))$ be the
 154 level of bacterial load, the per capita growth rate and the growth rate of bacteria
 155 within an individual at time $\tau \in (t_n, t_{n+1})$ and position $x_{a,b}$ respectively. We assume
 156 that the functions f and g depend on bacterial load $B(\tau, x_{a,b})$ so that f is negative
 157 when density of bacteria $B(\tau, x_{a,b})$ is small. Consequently $B(\cdot, x_{a,b})$ decreases when
 158 $B(t_n, x_{a,b}) < D(x_{a,b})$, increases when the initial condition $B(t_n, x_{a,b}) > D(x_{a,b})$ and
 159 is constant when $B(t_n, x_{a,b}) = D(x_{a,b})$ (see Figure 2(a)).

From (Jiang and Shi, 2009; Wang and Kot, 2001), g is written as function of f

(see Figure 2(b)) as:

$$g(B(\tau, x_{a,b})) = B(\tau, x_{a,b})f(B(\tau, x_{a,b}))$$

where

$$f(B(\tau, x_{a,b})) = \theta \left(\frac{B(\tau, x_{a,b})}{D(x_{a,b})} - 1 \right) \left(1 - \frac{B(\tau, x_{a,b})}{M} \right)$$

160 for all $\tau \in (t_n, t_{n+1})$, θ is the net growth rate of bacteria within an individual.

161 We assume the dynamics of individual bacterial load satisfies the following dif-
162 ferential equation:

$$\frac{dB(\tau, x_{a,b})}{d\tau} = g(B(\tau, x_{a,b})) + I_p(t_n, x_{a,b}), \quad \tau \in (t_n, t_{n+1}). \quad (1)$$

163 where initial condition of Eq. (1) is denoted by $B(t_n, x_{a,b})$. $I_p(t_n, x_{a,b})$ is interpreted
164 as the density of bacteria that an individual (i.e. all hens forming one individual)
165 acquires by ingestion or inhalation at time t_n and position $x_{a,b}$. We model the latter
166 in the form

$$I_p(t_n, x_{a,b}) = k \sum_{y_{i,j} \in \omega(r)} C(t_n, y_{i,j}). \quad (2)$$

167 where $\omega(r) \subset \Omega$ is the area of contamination around the individual at position $x_{a,b}$, k
168 is the transmission probability of infection of an individual after inhalation or inges-
169 tion of bacteria in environment. We have denoted by r the radius of contamination
170 around the individual of center x so that $\omega(r) := \{y \in \Omega : \|x - y\|_2 \leq r\}$ and $\|\cdot\|_2$
171 is the Euclidean norm.

172 The immune response is strongly dependant on many individual factors, e. g.
173 genetics (see for example Barrow, 2007; Bumstead and Barrow, 1988; Beaumont
174 et al., 2003). Therefore the individual threshold for bacterial load $D(x_{a,b})$, was
175 assumed to vary from an individual to another resulting in a variability between
176 individuals in the dynamics of Eq. (1) for the same initial condition $B(t_n, x_{a,b})$. Thus
177 we assume that the thresholds $D(\cdot)$ are triggered according to a random variable
178 Y_D defined by $Y_D = Z \times 10 \log_{10}$ where Z is beta distributed, $\mathcal{B}(p, q)$ ($p, q > 0$),
179 with mean $p/(p + q)$. Y_D takes on values in interval $(0, 10 \log_{10})$. For an individual
180 at position $x_{a,b}$, the threshold $D(x_{a,b})$ was drawn from distribution of Y_D at the
181 beginning of each replication and is kept constant during the replication.

182 2.7.2. Epidemiologic model

183 An individual located in position $x_{a,b}$ and at time step $\delta t = t_{n+1} - t_n$ is in one of the
184 five disease-states (see Figure 3): S_0 : susceptible individual without bacterial load.

Table 2: Baseline values for the parameters

	Description	Dimension	values
p, q	Parameters of beta distribution	Dimensionless	$p = 35, q = 45$
M	Carrying capacity of bacteria within an individual	cfu	$10 \log_{10}$
γ	Rate of transition from I_{D+} to I_S	Day ⁻¹	1/2
$\eta(B_{1x})$	Recovery rate	Day ⁻¹	Table 3
μ	Rate of return of individual from R to S_0 status	Day ⁻¹	1/200
$\beta_{I_{D+}}$	Excretion rate of individual at I_{D+} status.	Day ⁻¹	$4 \log_{10}$
β_{I_S}	Excretion rate of individual at I_S status.	Day ⁻¹	$4.5 \log_{10}$
λ	Natural death rate of <i>Salmonella</i> in environment.	Day ⁻¹	0.1
α^2	Diffusion coefficient of <i>Salmonella</i> in environment.	m ² × Day ⁻¹	0.01
k	Transmission probability of infection	Dimensionless	0.08
r	Radius of contamination around the individual	m	2
θ	Net growth rate of bacteria within an individual.	h ⁻¹	0.0007

185 I_{D-} : individual suffering from digestive infection at a dose lower than its threshold
 186 $D(x_{a,b})$ (i.e. with a transient infection). I_{D+} : individual suffering from digestive
 187 infection at a dose higher than its threshold $D(x_{a,b})$. I_S : individual systemically
 188 infected after the long term digestive infection. R : recovered individual. We denote
 189 by $\mathcal{H}(t_n, x_{a,b})$ the health state of an individual, $\mathcal{H}(t_n, x_{a,b}) \in \{S_0, I_{D-}, I_{D+}, I_S, R\}$.

190 Transitions from S_0 -state to I_{D-} -state and from I_{D-} -state to I_{D+} -state are only
 191 regulated by the density of bacteria within the individual. For each time-step δt , for
 192 each individual in S_0 -state or I_{D-} -state, we solve Eq. (1) via Runge Kutta methods
 193 (Butcher, 2003) and we obtain a unique solution denoted by $B(t_{n+1}, x_{a,b})$ for each
 194 initial condition $B(t_n, x_{a,b})$. We assume that for $B(t_{n+1}, x_{a,b}) = 0$, individual is in
 195 S_0 -state, when $B(t_{n+1}, x_{a,b}) \in]0, D(x_{a,b})$, individual is in I_{D-} -state and can go back
 196 to the S_0 -state. When the bacterial load $B(t_{n+1}, x_{a,b})$ becomes higher than the
 197 threshold $D(x_{a,b})$, then the individual changes its status from I_{D-} to I_{D+} state.
 198 The first occurrence of a bacterial load verifying, for an individual at position $x_{a,b}$,
 199 $B(t_{n+1}, x_{a,b}) > D(x_{a,b})$ is denoted by B_{1x} .

200 The transitions from I_{D+} -state to I_S -state, from I_S -state to I_R -state and from R -
 201 state to S_0 -state are stochastic. We denote by $T(x_{a,b}/I_{D+})$, $T(x_{a,b}/I_S)$ and $T(x_{a,b}/R)$,
 202 the residence time of an individual in the I_{D+} , I_S and R -state respectively. We
 203 assume that at time, t_n , an individual newly reaches the I_{D+} -state, $T(x_{a,b}/I_{D+})$ is

204 triggered according to an exponential distribution with an average duration equal to
 205 $1/\gamma$ and the individual will change its status from I_{D+} to I_S at time, $t_{n+\ell}$, where ℓ
 206 equal to the integer part of $T(x_{a,b}/I_{D+})/\delta t$. In the same way, successively $T(x_{a,b}/I_S)$
 207 and $T(x_{a,b}/R)$ are triggered according to an exponential distribution with an average
 208 duration equal to $1/\eta(B_{1x})$ and $1/\mu$. We denote by $P_{I_{D+}}$, P_{I_S} and P_R respectively,
 209 the transition probabilities for I_{D+} to become I_S , I_S to become R , R to become S_0
 210 per unit of time. Then $(P_{I_{D+}}, P_{I_S}, P_R) = (1 - \exp(-1/\gamma), 1 - \exp(-1/\eta(B_{1x})), 1 -$
 211 $\exp(-1/\mu))$.

212 2.7.3. Model for diffusion of bacteria in the hen house

213 Bacterial environmental contamination within an industrial hen house is mod-
 214 eled assuming that *Salmonella* is dispersed in the environment via a diffusion process
 215 through dust particles and contaminated aerosols (Gast et al., 2002; Nakamura et al.,
 216 1994; Lever and Williams, 1996). Let $C_{i,j}^n = C(t_n, x_{i,j})$ be the density of bacteria
 217 at time t_n and position $x_{i,j}$. $C_{i,j}^n$ is a approximated solution of a continuous reac-
 218 tion diffusion equation describing the dispersion of bacteria in hen house (Appendix
 219 Eq. (A.1)). It was approximated by a forward finite difference scheme in time and
 220 centered finite difference scheme in space, which gives

$$\begin{aligned} \frac{C_{i,j}^{n+1} - C_{i,j}^n}{\delta t} &= \frac{\alpha^2}{(\delta x_1)^2} (C_{i+1,j}^{n+1} - 2C_{i,j}^{n+1} + C_{i-1,j}^{n+1}) \\ &+ \frac{\alpha^2}{(\delta x_2)^2} (C_{i,j+1}^{n+1} - 2C_{i,j}^{n+1} + C_{i,j-1}^{n+1}) \\ &- \lambda C_{i,j}^{n+1} + (\beta_{I_S})_{i,j}^{n+1} + (\beta_{I_{D+}})_{i,j}^{n+1} \end{aligned} \quad (3)$$

with boundary conditions

$$C_{0,j}^{m+1} = C_{1,j}^{m+1}, C_{N_1-1,j}^{m+1} = C_{N_1,j}^{m+1},$$

$$C_{i,0}^{m+1} = C_{i,1}^{m+1}, C_{i,N_2-1}^{m+1} = C_{i,N_2}^{m+1},$$

221 and initial condition $C_{i,j}^0 \geq 0$. Convergence of numerical scheme in $\|\cdot\|_\infty$ norm
 222 is obtained by the following condition $\delta t \alpha^2 / (\delta x_1)^2 < 1/4$ and $\delta t \alpha^2 / (\delta x_2)^2 < 1/4$
 223 (Lucquin and Pironneau, 1996, Page 281).

224 2.8. Calibration

225 *Data for carrying capacity M*: we have no data to estimate the value of M .
 226 Noticing that in experimental infections, almost all individuals are infected with
 227 an inoculum dose ranging between $3 \log_{10}$ and $9.5 \log_{10}$ colony-forming units (cfu)

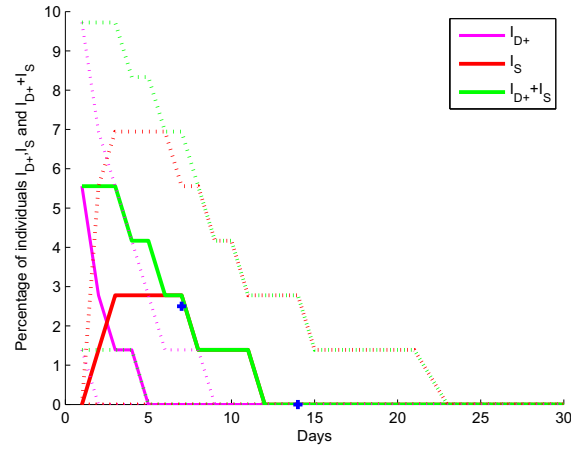
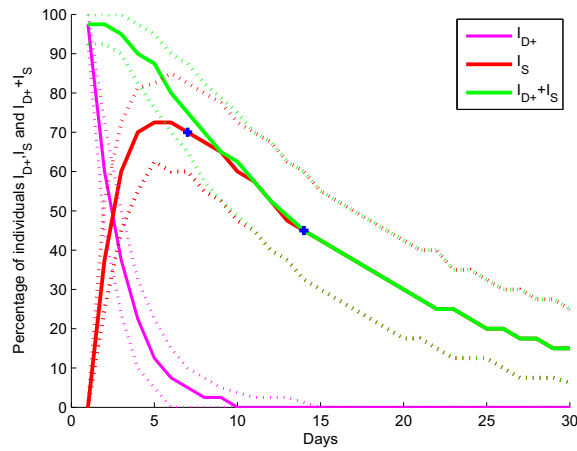
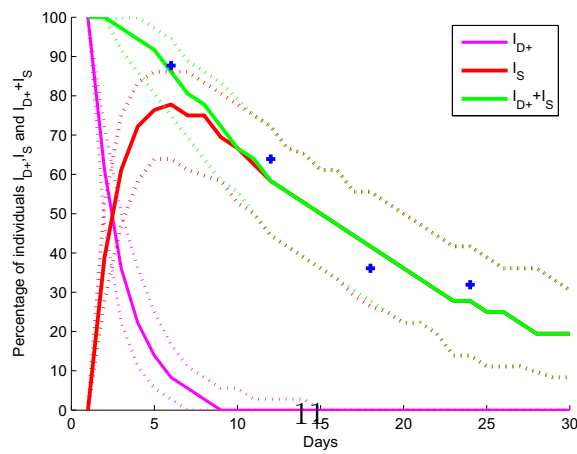
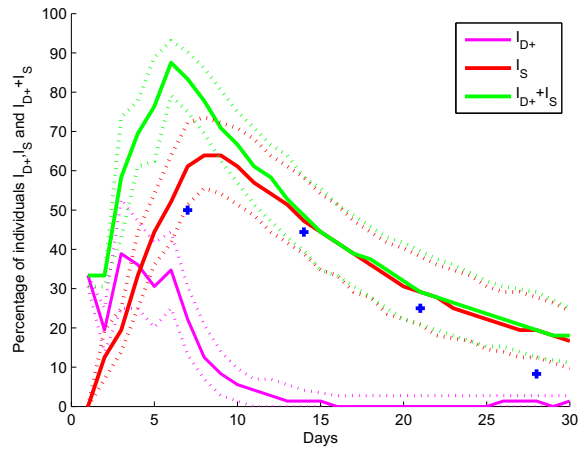
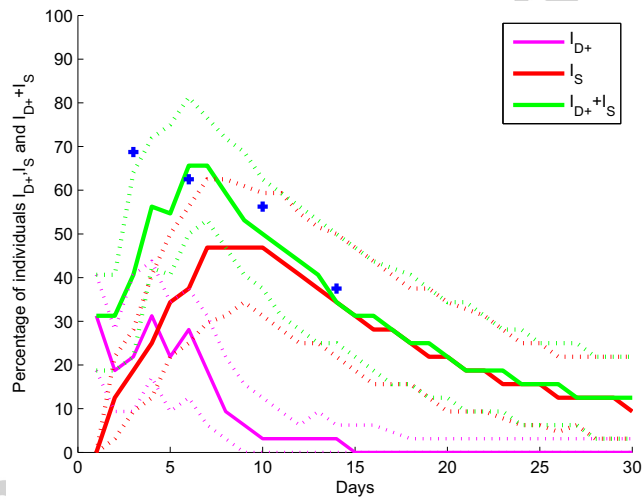
(a) Dose= 10^4 cfu(b) Dose= 10^6 cfu(c) Dose= $7.5 \cdot 10^7$ cfu

Figure 4: Evolution over time of the percentages of I_{D+} , I_S and $I_{D+} + I_S$ when all individuals were inoculated with the same bacterial dose a) $= 10^4$ cfu and b) $= 10^6$ cfu as in Gast (1993); c) $= 7.5 \cdot 10^7$ cfu as in Gast et al. (1997). Observed data (corresponding to percentage of individuals shedding Salmonella in feces) are shown by crosses. Median value of simulations are shown by solid lines. The 5th and 95th percentiles observed on the 300 replicates are shown by dotted curves.

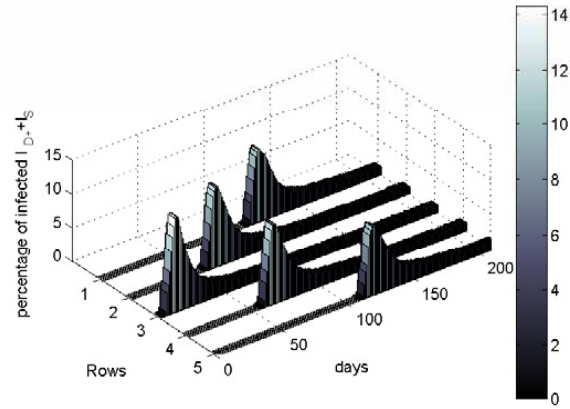


(a)

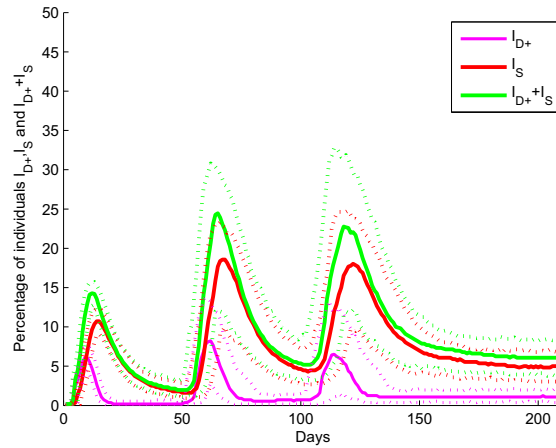


(b)

Figure 5: Evolution over time of the percentages of I_{D+} , I_S and $I_{D+} + I_S$ after rearing infected individuals in the vicinity of healthy ones a) i.e inoculating (10^6 cfu) one single individual out of three as in Gast (1993) and b) letting 8 infected (10^5 cfu) as in Nakamura et al. (1994). In both cases, individuals are in two adjacent rows and inoculated individuals share water with not uninoculated ones. Observed data (corresponding to percentage of individuals shedding Salmonella in feces) are shown by crosses. Median value of simulations are shown by solid lines. The 5th and 95th percentiles observed on the 300 replicates are shown by dotted curves.

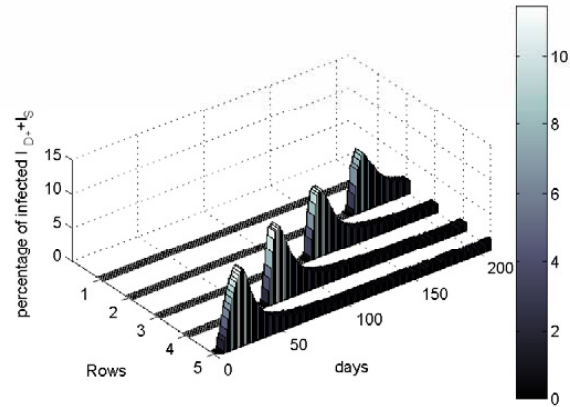


(a) Evolution of the percentage of $I_{D+} + I_S$ over time and row

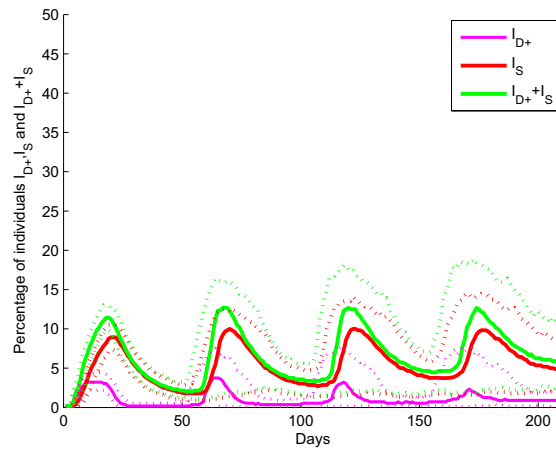


(b) Evolution of the percentage of I_{D+} , I_S and $I_{D+} + I_S$ over time

Figure 6: Results of simulations achieved using data from Table 4 (column (g)) and inoculation of one individual at Day 0 with a high bacterial dose (10^9 cfu) in the midst of hen house, when rows are separated from each other by 2 meters. (a): only the median value on the 300 replicates are shown, (b): median value of simulations are shown by solid lines. The 5th and 95th percentiles observed on the 300 replicates are shown by dotted curves.

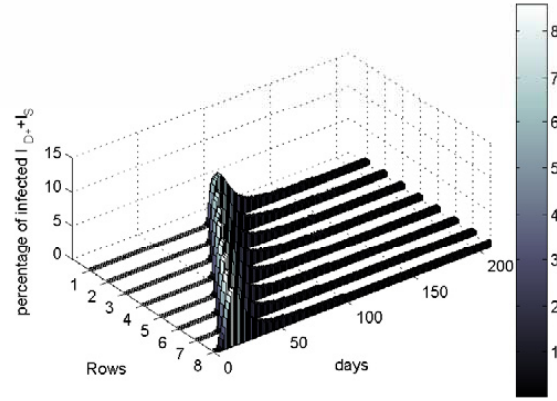


(a) Evolution of the percentage of $I_{D+} + I_S$ over time and row

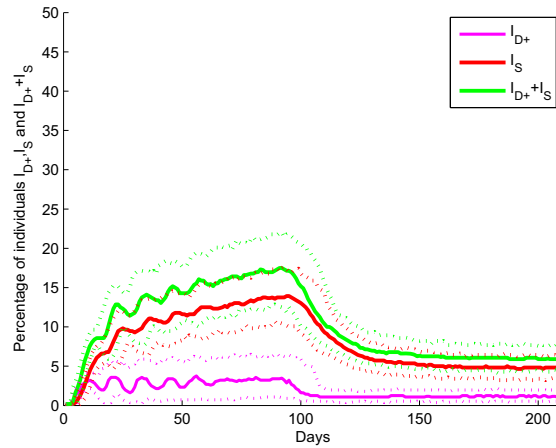


(b) Evolution of the percentage of I_{D+} , I_S and $I_{D+} + I_S$ over time

Figure 7: Results of simulations achieved using data from Table 4 (column (g)) and inoculation of one individual at Day 0 with a high bacterial dose (10^9 cfu) at the corner of hen house, when rows are separated from each other by 2 meters. (a): only the median value on the 300 replicates are shown, (b): median value of simulations are shown by solid lines. The 5th and 95th percentiles observed on the 300 replicates are shown by dotted curves.



(a) Evolution of the percentage of $I_{D+} + I_S$ over time and row



(b) Evolution of the percentage of I_{D+} , I_S and $I_{D+} + I_S$ over time

Figure 8: Results of simulations achieved using data from Table 4 (column (f)) and inoculation of one individual at Day 0 with a high bacterial dose (10^9 cfu) at the corner of hen house, when rows are separated from each other by 1 meter. (a): only the median value on the 300 replicates are shown, (b): median value of simulations are shown by solid lines. The 5th and 95th percentiles observed on the 300 replicates are shown by dotted curves.

Table 3: Calibration of the average duration of the systemic period, $1/\eta(B_{1x})$ as a function of B_{1x} (the first value of $B(t_{n+1}, x_{a,b})$ satisfying $B(t_{n+1}, x_{a,b}) > D(x_{a,b})$).

B_{1x} in cfu	$< 10^4$	$[10^4, 5 \cdot 10^4[$	$[5 \cdot 10^4, 10^5[$	$[10^5, 5 \cdot 10^5[$	$[5 \cdot 10^5, 10^6[$	$> 10^6$
$1/\eta(B_{1x})$ in day	1	4	7	10	13	16
$1/\eta(B_{1x}) + 1/\gamma$ in day	3	6	9	12	15	18

228 and that a saturation of bacteria within an individual seems to be observed be-
 229 yond $9.5 \log_{10} cfu$ (Gast, 1993; Gast et al., 2004; Humphrey et al., 1991; Lever and
 230 Williams, 1996), M was set at $10 \log_{10} cfu$.

231 *Data for recovery rate, η and rate of transition from I_{D+} to I_S , γ :* Humphrey
 232 et al. (1991, Table 1) showed that the duration of faecal excretion is correlated with
 233 the size of inoculum dose and can vary from 3.4 to 36.8 days for dose varying from 10^3
 234 to 10^6 while Gast et al. (2005) showed that the duration of faecal excretion can vary
 235 from 13.8 to 32.9 for an inoculum dose at 10^9 of different *Salmonella* strains. Since
 236 individuals excrete at digestive or systemic state, the sum of average durations of the
 237 digestive period, $1/\gamma$, and of the systemic period, $1/\eta$ is necessarily a function of the
 238 inoculum size and of the *Salmonella* strains. Setting $1/\gamma$ at 2 days as in (Prévost
 239 et al., 2006, 2008), then we generate some residence time in I_{D+} varying in about 95%
 240 of the simulation from 0.05 to 3 days. Assuming that $1/\eta(B_{1x})$ depends on the initial
 241 value of bacterial load in I_{D+} -status, mean $1/\eta(B_{1x})$ was calibrated as described in
 242 Table 3. This allowed to generate with exponential distribution residence time in I_S
 243 varying in 95% of the simulations from 0.6 to 47 days for doses ranging from 10^3 to
 244 10^9 .

245 *Data for parameters p and q of beta distribution to trigger the individual threshold*
 246 $D(x_{a,b})$: we set $p = 35$ and $q = 45$ so that 5% of individuals have a bacterial threshold
 247 lower than $3.5 \log_{10}$ and higher than $5.8 \log_{10}$.

248 *Data for net growth θ :* the net growth rate is the key parameter influencing
 249 simultaneously the fast-growing (or slow-growing) and the fast-decreasing (or slow-
 250 decreasing) of the bacterial load over time when the initial bacterial load is higher
 251 and lower respectively than the threshold. Many factors such as the bacterial strain,
 252 host factors might affect this parameter. In the literature, no experimental data were
 253 available for laying hens. We assumed that θ is equal to $0.0007 h^{-1}$.

254 *Data for mortality rate of bacteria λ :* we assume that the mortality rate of bac-
 255 teria in the environment is $\lambda = 0.1 day^{-1}$ as (Prévost et al., 2006, 2008).

256 *Rate of bacterial excretion for I_{D+} and I_S states:* as in Prévost et al. (2006, 2008),

257 we assumed that individuals excreted low levels of bacteria and that an individual in
 258 I_{D+} excreted less than an individual in I_S state. We set $\beta_{I_{D+}} = 4 \log_{10} \text{cfu} \times \text{Day}^{-1}$,
 259 and $\beta_{I_S} = 4.5 \log_{10} \text{cfu} \times \text{Day}^{-1}$.

260 *Data for transmission probability of infection of an individual after inhalation*
 261 *or ingestion of bacteria, k , and radius of contamination around the individual, r :*
 262 from Eq. (1), variation in parameters k or r will result in a similar trend in the the
 263 density of bacteria that an individual (i.e. all hens forming one individual) acquires
 264 by ingestion or inhalation (I_P). To calibrate these data, we used the results for
 265 the inhalation dose of bacteria calculated by Lever and Williams (1996) in rearing
 266 conditions similar to that of flock of laying hens. These results showed that each
 267 individual would inhale every 24 h a bacterial load ranging between 0 and $2 \log_{10}$.
 268 We assumed that $r = 2$ m (maximal distance for aerosol transmission) and k was set
 269 at 0.08 so that I_P remains in the interval $(0, 2 \log_{10})$.

270 *Data for diffusion coefficient α^2 :* we assumed that α^2 is equal to 0.01.

271 3. Simulation experiments

272 3.1. Material and method

273 Three types of scenarios are considered, the first two for model validation and
 274 the third for model exploration. The width, L_2 and length, L_1 of hen house were
 275 always initialized to 15 m and 30 m respectively while the number of individuals
 276 varies following the scenarios and are summarized in Table 4. To quantify the level
 277 of agreement between predicted and simulated data, the Standard error of simulated
 278 and observed data was evaluated for the scenarios 1 and 2.

279 3.1.1. Scenario 1: validation of kinetics of infection

280 Experiments in which all individuals were initially inoculated with the same dose
 281 of bacteria were considered. In that case, reinfection between individuals was reduced
 282 as much as possible (by rearing with individual food and water). That was the
 283 case of the first experiment described by Gast (1993) where 40 individuals were
 284 considered (Table 4 (a) and (b)) and an another experiment described by Gast et al.
 285 (1997) where 36 individuals were considered (Table 4 (c)). In both cases, all of them
 286 were inoculated at Day 0. Three bacterial doses, 10^4 cfu, 10^6 cfu and $7.5 \cdot 10^7$ cfu
 287 were studied (one per replicate) and infections were regularly investigated on feces
 288 samples. As individuals excrete *Salmonella* in feces in I_{D+} and I_S -state, the observed
 289 prevalence were compared to the simulated percentages $I_{D+} + I_S$. The percentages
 290 of I_S were also considered to investigate the repartition between the two status. A
 291 total of 300 simulations were achieved with the same dose and the same number of
 292 individuals.

293 Since transmission via the environment was very low if any and can be neglected,
 294 the value of the parameter k in Eq. (2) was set equal to zero.

295 *3.1.2. Scenario 2: validation of the Salmonella spread from individuals to individuals*
 296 *via the environment*

297 We selected for model validation two experiments where experimentally infected
 298 individuals were reared with healthy ones. Gast (1993) studied a total of 72 individ-
 299 uals where he inoculated one-third of them (i.e. every 3rd individual) with a dose of
 300 bacteria at 10^6 cfu. Nakamura et al. (1994) infected 8 individuals out of 16 (i.e. every
 301 2nd individual) with a dose of bacteria at 10^5 cfu. The latter precisely described the
 302 distribution of individuals considering one pair of adjacent rows (i.e. 8 individuals
 303 in one row share drinking water with adjacent individuals) Table 4 (e). First four
 304 individuals was inoculated in one row and last four individuals in the second row at
 305 the beginning of experiment. At the opposite, the former gave no information on
 306 the spatial distribution of individuals but only the route of cross contamination was
 307 known (uninoculated individuals shared drinkers and feeders with inoculated ones).
 308 We therefore assumed that the individuals were housed in one pair of rows as in
 309 Nakamura et al. (1994) (Table 4 (d)). Since in both experiments, Salmonella were
 310 searched in feces and our model assumes that excretion occurs in the I_S or $I_{D+} + I_S$
 311 state, results must be compared to the sum of I_{D+} and I_S individuals. However,
 312 since the rate of excretion is five-fold higher in the systemic state, comparison with
 313 number of hens in the Systemic state was also considered. As in scenario 1, observed
 314 and simulated percentages of $I_{D+} + I_S$ and I_S were compared. For simulations, a
 315 total of 300 simulations were achieved.

316 *3.1.3. Standard error of simulated and observed data*

317 In scenario 1 and 2, we evaluate the root mean squared error ($RMSE$) known as
 318 the standard error of simulated and observed data.

$$RMSE := \sqrt{\frac{\sum_{l=1}^N (obs(t_l) - sim(t_l))^2}{N}} \quad (4)$$

319 where N is the number of observed data, $obs(t_l)$ and $sim(t_l)$ are the observed and
 320 simulated data at time t_l respectively. $RMSE$ has the same units that the simulated
 321 and observed data which are in percentage.

322 *3.1.4. Scenario 3: influence of the position of the first infection and the distance*
 323 *between pair of rows in the hen house*

324 To investigate the influence of the position of the first infection, initialization of
 325 hen house was achieved as described in the Table 4(f). Two cases were considered

326 according to this infection occurred either in one corner (i.e. in pair of row 5) or on
 327 the middle (i.e. pair of row 3) of the hen house. In both cases, only one individual
 328 was infected on Day 0 with a high dose (10^9 cfu).

329 The effect of the spatial distribution of individuals in hen house was also consid-
 330 ered by comparing results with data from scenario in Table 4(f) or (g). In the former
 331 case, the distance between pair of row is 2 m versus 1 in the latter.

332 A total of 300 simulations were achieved and the simulated percentages of I_S or
 333 $I_{D+} + I_S$ was represented.

334 3.2. Results

335 3.2.1. Scenario 1: validation of kinetics of infection

336 Results obtained when simulating data and those observed after experimental
 337 inoculation are shown on Figure 4a to 4c for doses of 10^4 cfu, 10^6 cfu and $7.5 \cdot 10^7$ cfu
 338 respectively. Simulated percentage of $I_{D+} + I_S$ and observed results are very close
 339 for the three doses (see Table 5(a), (b) and (c) for $I_{D+} + I_S$) and lay between the 5th
 340 and 95th percentiles. Simulated percentages of I_S are also very close to observation
 341 made at the first two doses (see Table 5(a) and (b) for I_S). For the highest dose
 342 however, the observation obtained one week post inoculation is close but higher than
 343 the 95th percentile (see Table 5(c) for I_S).

344 3.2.2. Scenario 2: validation of the Salmonella spread from individuals to individuals 345 via the environment

346 Simulated percentages of I_S or $I_{D+} + I_S$ and observed prevalence from experiments
 347 are shown in Figure 5a for the experiment of Gast (1993) and Figure 5b for the
 348 experiment of Nakamura et al. (1994).

349 In the former the greatest disagreement between any of the data sets and sim-
 350 ulated percentage of infected individuals was found with regards to $I_{D+} + I_S$ see
 351 table 5(d). This is especially true for data obtained one week post inoculation (p.i.)
 352 while later on both sets of results were very close.

353 In the latter case, observed results lay between the 5th and 95th percentiles of
 354 simulated percentage of $I_{D+} + I_S$ except for the observation obtained three days post
 355 inoculation which is close to the 95th percentile. When simulated percentage of I_S
 356 is considered, differences are larger. Observed data at 3 and 6 days p.i. were much
 357 higher than simulated percentage of I_S : the former ranged from 68.7 to 62.5% while
 358 median percentage of I_S varied from 19 to 40%. Comparing results on Table 5(e),
 359 $I_{D+} + I_S$ fits observed data better than I_S .

Table 4: Initialisation of individuals in hen house for each scenario.

Description	Scenario 1			Scenario 2		Scenario 3	
	(a)	(b)	(c)	(d)	(e)	(f)	(g)
Inoculum dose in cfu	10^4	10^6	$7.5 \cdot 10^7$	10^6	10^5	10^9	10^9
Number of pair of rows	1	1	1	1	1	8	5
Number of individuals per row	20	20	18	36	8	35	56
Number of individuals	40	40	36	72	16	560	560

Table 5: Standard error in percentage using I_S versus $I_S + I_{D+}$ as simulated data.

Description	Scenario 1			Scenario 2	
	(a)	(b)	(c)	(d)	(e)
Standard error for I_S	0.19	1.67	6.65	8.26	28.38
Standard error for $I_S + I_{D+}$	0.19	4.78	4.51	17.82	14.57

360 *3.2.3. Scenario 3: influence of the position of the first infection and of the distance*
 361 *between pair of rows in the hen house*

362 Influence of the position of the first infection is illustrated on the figures 6 and
 363 7 respectively for a first occurrence in the middle and in the corner of the hen
 364 house respectively. The position of the first infection influences both the kinetics of
 365 infection and the maximal percentages of infected individuals. As late as 210 days
 366 post inoculation, the first pair of rows is still not colonized for an infection starting
 367 in the opposite corner (see Figure 7a) while when the infection starts in the middle,
 368 all five pair of rows are infected about 210 days post inoculation (see Figure 6a).
 369 The infection starting in the middle of the hen house results in a higher maximal
 370 of percentage of $I_S + I_{D+}$ than an infection starting at a corner: 25% versus 13%
 371 (Figures 6b and 7b, 70 days post inoculation).

372 Influence of the distance between pair of rows in the hen house (1 m versus 2 m)
 373 can be seen by comparing the figures 8 and 7. When the pair of rows are close, the
 374 colonization is rapid with a lower maximal of percentage of $I_S + I_{D+}$: for example all
 375 eight pair of rows are infected about 110 days post inoculation (see Figure 8a) with
 376 maximal percentage of $I_S + I_{D+}$ of 17.5% at 100 days post inoculation (see Figure 8b).
 377 At the opposite, the colonization is slow with a close maximal percentage of $I_S + I_{D+}$
 378 but a lower minimal percentage.

379 **4. Discussion**

380 This model extends the previous model derived by Prévost et al. (2006) where
381 individuals infected at the digestive level were only distinguished from those infected
382 at the systemic level. Here, individuals in the I_{D-} status may overcome the bacterial
383 infection as long as the bacterial load remains lower than the $D(x_{a,b})$ threshold. At
384 the opposite, when the individual bacterial dose is higher than $D(x_{a,b})$, individuals
385 change to the I_{D+} status and undergo a longer term infection.

386 The threshold, $D(x_{a,b})$, which is the maximal bacterial load that the individual
387 may clear without persistent and systemic infection, depends on many factors such as
388 the bacterial strain (as can be seen for example from Bumstead and Barrow, 1988),
389 gut flora (Rantala and Nurmi, 1973), individuals' genetic resistance (see for example
390 Beaumont et al. (2009)). The threshold was thus chosen as random. In practice,
391 the balance between bacterial doses and individuals threshold will be determinant
392 in the propagation of *Salmonella*, since in the field bacterial doses are most often
393 rather small. Introducing this threshold thus allows investigating the effects of both
394 average values and variability of these factors.

395 In the model immune response was considered only through its impact on the
396 bacterial load, without refining the description of biological processes which are far
397 too complex (see for example Host, 2000) to be modeled at the same time as the
398 whole flock is considered. Moreover, parametrization of the immunity response would
399 have been hardly feasible because of large number of biological steps that may be
400 considered. This would have led to the introduction of a higher uncertainty on the
401 process that would decrease the confidence on the model results. Using the strong
402 allee effect, only three parameters were needed: net growth rate of bacterial within
403 the individual, θ , the individual threshold of bacterial load corresponding to the
404 balance between bacterial multiplication within the host and host response leading
405 to bacterial clearance by immune response, $D(x_{a,b})$ and the carrying capacity M .
406 All three of them have a biological meaning which facilitated their estimation and
407 allowed to base it on experimental data: the threshold $D(x_{a,b})$ and carrying capacity
408 were chosen from numerous results of experimental infections where individuals are
409 infected with inoculum doses ranging between $3 \log_{10}$ and $9.5 \log_{10}$ colony-forming
410 units (cfu) (Humphrey et al., 1991; Gast, 1993; Lever and Williams, 1996; Gast
411 et al., 2004). Large differences in prevalence even in the first days after inoculation
412 were observed when the dose were higher or lower than $5 \log_{10}$ leading us to choose
413 this value as the average value for the threshold.

414 Variations in durations of bacterial clearance were also considered, taking advantage
415 of experimental data obtained in Humphrey et al. (1991); Gast et al. (2005).
416 Indeed, this duration was shown by Prévost et al. (2008) to be partly under a genetic

417 control. Preliminary investigations showed that this duration had a large impact on
418 kinetics of colonization, especially at longer intervals post inoculation.

419 This model allows reproducing experimental results. Indeed, the simulated per-
420 centages and observed data are very coherent when experimental inoculations are
421 considered. They are also consistent with observations resulting from infection be-
422 tween individuals via environment, although simulations overestimated the outcome
423 compared to the second experiment by Gast (1993) where the spatial distribution of
424 individuals in the hen house was unknown. As the spatial distribution of individuals
425 such as the distance between pair of rows influences both the kinetics of infection and
426 the maximal percentages of infected individuals (see scenario 3), it might explain the
427 disagreement between experimental and simulated data. Moreover, no experimental
428 data were available for the first six days post-inoculation for model validation as in
429 Nakamura et al. (1994).

430 Distinguishing individuals I_S and I_{D+} allows to understand what happens during
431 the first days post inoculation. At the opposite, the sum $I_{D+} + I_S$ gives the real
432 prevalence of infection since fecal samples may found be negative even in the case of
433 caecal infection. The differences between both sets of data disappear at longer post
434 inoculation intervals. Then only systemically infected individuals may be observed
435 so that both simulations and observations refer to the same category of individuals.

436 Moreover, this model makes it possible to study the spatial diffusion of the bac-
437 teria and disease, while until now, to our knowledge at least, no data or model were
438 available to study spatial diffusion of *Salmonella* or any other pathogenic agents in
439 a hens' flock.

440 Most studies showed that flock size has an effect on the prevalence of *Salmonella*
441 within a laying flock (EFSA, 2009; Huneau-Salaun et al., 2009; Carrique-Mas et al.,
442 2009) but the influence of the position of the first infection or the distance between
443 pair of rows in hen house may have an important effect in the prevalence (see sce-
444 nario 3). Our results show that these assumptions are exact and that the speed of
445 colonization may depend on the position of the first infection.

446 However, the model considers all hens in a cage as an epidemiological unit. In-
447 deed, most often all of them will be infected at the same time (by contaminated feed,
448 water, rodent...) and/or cross infected through aerosols contamination via excreted
449 bacteria of the environment (among which food and drinkers).

450 This model will make it possible to investigate new strategies of reduction of
451 *Salmonella* prevalence. That will be the case for the spatial effect of introducing more
452 resistant individuals. (Prévost et al., 2008) showed that introducing a proportion of
453 more resistant fowls, assuming a homogenous mixing of the two subpopulations of
454 resistant and of susceptible individuals resulted in a reduction of the overall propor-

455 tion of infected fowls. With our model, we will be able to study possible effects of
 456 the relative spatial positions of susceptible and resistant individuals on the spatial
 457 spread of the *Salmonella* in hen house. Considering individual variations in bacterial
 458 threshold and duration of clearance will also make it possible to study possible effects
 459 of differences in excretion rates which may have a major impact on environmental
 460 contamination.

461 5. Conclusion

462 In this article, we formulated an individual-based model to describe the spread
 463 of *Salmonella* within a laying flock. This is the first stochastic model describing
 464 *Salmonella* spatio-temporal spread within a poultry flock. It is able to repro-
 465 duce experimental data; the conceptual understanding of environmental mediated
 466 Salmonella spread appears complete. It will thus allow studying the interest of var-
 467 ious prophylactic means against this disease as well as the effect of changes or vari-
 468 ability of various factors. The model could also be adapted to study the propagation
 469 of other pathogens within laying hens.

470 Acknowledgements

471 This study was achieved with a grant from the EADGENE network of Excellence.
 472 Pascal Zongo has a post-doctoral grant from the EADGENE network of Excellence
 473 and INRA. The authors would like to thank the two anonymous referees for many
 474 helpful suggestions.

475 Appendix A. Continuous formulation of sub-model 2.7.3

476 Let $C(t, x)$ be the density of bacteria in the environment at time t and position
 477 $x = (x_1, x_2) \in \Omega$, $t \geq 0$. $C(t, x)$ depends on the initial contamination, $C(0, x) \geq 0$,
 478 bacterial diffusion rate, α^2 , and mortality rate, λ , as well as on excretion rate, $\beta_{I_{D+}}$,
 479 and, β_{I_S} , by individuals at I_{D+} and I_S -state respectively. The density dynamics
 480 satisfies the following equation:

$$\frac{\partial C(t, x)}{\partial t} = \alpha^2 \Delta_x C(t, x) - \lambda C(t, x) + \beta_{I_S}(x) + \beta_{I_{D+}}(x) \quad (\text{A.1})$$

481 where $\Delta_x = \partial^2/\partial x_1^2 + \partial^2/\partial x_2^2$, with no flux boundary condition $\partial C(t, x)/\partial \nu = 0$ on
 482 $\partial\Omega$, ν is the outward normal. $\beta_{I_S}(x) = 0$ if at position x there is no individual at
 483 I_{D+} -state; $\beta_{I_{D+}}(x) = 0$ if at position x there is no individual at I_S -state. We assume
 484 that $\beta_{I_{D+}}$ and β_{I_S} are constant. Therefore their values are uniformly distributed in
 485 the area covered by the individual during excretion.

486 **References**

- 487 Barrow, P.A., 2007. *Salmonella* infections: immune and non-immune protection with
488 vaccines. *Avian Pathol.* 36, 1–13.
- 489 Beaumont, C., Chapuis, H., Protais, J., Sellier, N., Menanteau, P., Fravallo, P.,
490 Velge, P., 2009. Resistance to *Salmonella* carrier-state: selection may be efficient
491 but response depends on animal's age. *Genet. Res.* 91, 161–169.
- 492 Beaumont, C., Dambrine, G., Chaussé, A.M., Flock, D., 2003. Selection for disease
493 resistance: conventional breeding for resistance to bacteria and viruses, in Muir,
494 W. M. and Aggrey, S. E. (Eds.), *Poultry Genetics, Breeding and Biotechnology.*
495 CAB, Publishing, Wellingford, 357-384.
- 496 Bumstead, N., Barrow, P.A., 1988. Genetics of resistance to *Salmonella* typhimurium
497 in newly hatched chicks. *Brit. Poultry Sci.* 29, 521–529.
- 498 Butcher, J.C., 2003. *Numerical Methods for ordinary differential equations.* John
499 Wiley & Sons. hardbound edition.
- 500 Carrique-Mas, J.J., Breslin, M., Snow, L., McLaren, I., Sayers, A.R., Davies, R.H.,
501 2009. Persistence and clearance of different *Salmonella* serovars in buildings hous-
502 ing laying hens. *Epidemiol. Infect.* 137, 837–846.
- 503 EFSA, 2009. The community summary report on food-borne outbreaks in the euro-
504 pean union in 2007. *The EFSA J.* , 271.
- 505 Gast, R.K., 1993. Detection of *Salmonella* enteritidis in experimentally infected
506 laying hens by culturing pools of egg contents. *Poultry Sci.* 72, 267–274.
- 507 Gast, R.K., Guard-Bouldin, J., Holt, P.S., 2004. Colonization of reproductive organs
508 and internal contamination of eggs after experimental infection of laying hens with
509 *Salmonella* heidelberg and *Salmonella* enteritidis. *Avian Dis.* 48, 863–869.
- 510 Gast, R.K., Guard-Bouldin, J., Holt, P.S., 2005. The relationship between the du-
511 ration of fecal shedding and the production of contaminated eggs by laying hens
512 infected with strains of *Salmonella* enteritidis and *Salmonella* heidelberg. *Avian*
513 *Dis.* 49, 382–386.
- 514 Gast, R.K., Guard-Petter, J., Holt, P.S., 2002. Characteristics of *Salmonella* en-
515 teritidis contamination in eggs after oral, aerosol, and intravenous inoculation of
516 laying hens. *Avian Dis.* 46, 629–635.

- 517 Gast, R.K., Porter, R.E., Holt, P.S., 1997. Applying tests for specific yolk antibodies
518 to predict contamination by *Salmonella* enteritidis in eggs from experimentally
519 infected laying hens. *Avian Dis.* 41, 195–202.
- 520 Grijspeerdt, K., Kreft, J.U., Messens, W., 2005. Individual-based modelling of
521 growth and migration of *Salmonella* enteritidis in hens'eggs. *Int. Journal Food*
522 *Microbiol.* 100, 323–333.
- 523 Grimm, V., Berger, U., Bastiansen, F., Eliassen, S., Ginot, V., et al., 2006. A
524 standard protocol for describing individual-based and agent-based models. *Ecol.*
525 *Model.* 198, 115–126.
- 526 Hill, A.A., Snary, E.L., Arnold, M.E., Alban, L., Cook, A.J., 2008. Dynamics of
527 *Salmonella* transmission on a British pig grower-finisher farm: a stochastic model.
528 *Epidemiol. Infect.* 136, 320–333.
- 529 Host, P.S., 2000. Host Susceptibility, Resistance and Immunity to *Salmonella* in
530 Animals in: Wray, C. and Wray, A. (Eds.), *Salmonella* in Domestic Animals.,
531 CAB, Publishing, New York.
- 532 Humphrey, T.J., 1990. Public health implications of infection of egg-laying hens with
533 *Salmonella* enteritidis phage typ 4. *World's Poultry Sci. J.* 46, 5–13.
- 534 Humphrey, T.J., Baskerville, A., Chart, H., Rowe, B., Whitehead, A., 1991.
535 *Salmonella* enteritidis PT4 infection in specific pathogen free hens: influence of
536 infecting dose. *Vet. Rec.* 129, 482–485.
- 537 Humphrey, T.J., Lanning, D.G., 1988. The vertical transmission of *Salmonella* and
538 formic acid treatment of chicken feed. A possible strategy for control. *Epidemiol.*
539 *Infect.* 100, 43–49.
- 540 Huneau-Salaun, A., Chemaly, M., Bouquin, S., Lalande, F., Petetin, I., Rouxel, S.,
541 Michel, V., Fravallo, P., Rose, N., 2009. Risk factors for *Salmonella* enterica subsp.
542 enterica contamination in 519 French laying hen flocks at the end of the laying
543 period. *Prev. Vet. Med.* 89, 51–58.
- 544 Ishola, O.O., 2009. Effects of challenge dose on faecal shedding of salmonella enteri-
545 tidis in experimental infected chickens. *Afr. J. Biotechnol.* 8, 1343–1346.
- 546 Jiang, J., Shi, J., 2009. Bistability dynamics in some structured ecological models,
547 in Cantrell, S., Cosner, C. and Ruan S. (Eds.), *Spatial Ecology*. CRC Press.

- 548 Lanzas, C., Brien, S., Ivanek, R., Lo, Y., Chapagain, P.P., Ray, K.A., Ayscue, P.,
549 Warnick, L., Gröhn, Y.T., 2008. The effect of heterogeneous infectious period
550 and contagiousness on the dynamics of *Salmonella* transmission in dairy cattle.
551 *Epidemiol. Infect.* 136, 1496–1510.
- 552 Leslie, J., 1996. Simulation of the transmission of *Salmonella* enteritidis phage type
553 4 in a flock of laying hens. *Vet. Rec.* 139, 388–391.
- 554 Lever, M.S., Williams, A., 1996. Cross-infection of chicks by airborne transmission
555 of *Salmonella* enteritidis PT4. *Lett. Appl. Microbiol.* 23, 347–349.
- 556 Lucquin, B., Pironneau, O., 1996. Introduction au calcul scientifique. Masson, Paris.
- 557 Lurette, A., Belloc, C., Touzeau, S., Hoch, T., Ezanno, P., Seegers, H., Fourichon,
558 C., 2008. Modelling *Salmonella* spread within a farrow-to-finish pig herd. *Vet.*
559 *Res.* 39, 1–12.
- 560 Nakamura, M., Nagamine, N., Takahashi, T., Suzuki, S., Kijima, M., Tamura, Y.,
561 Sato, S., 1994. Horizontal transmission of *Salmonella* enteritidis and effect of stress
562 on shedding in laying hens. *Avian Dis.* 38, 282–288.
- 563 Prévost, K., Magal, P., Beaumont, C., 2006. A model of *Salmonella* infection within
564 industrial house hens. *J. Theor. Biol.* 242, 755–763.
- 565 Prévost, K., Magal, P., Protais, J., Beaumont, C., 2008. Effet of genetic resistance of
566 hen to *Salmonella* carrier-state on incidence of bacterial contamination : synergy
567 with vaccination. *Vet. Res.* 38, 1–20.
- 568 Rantala, M., Nurmi, E., 1973. Prevention of the growth of *Salmonella* infantis in
569 chicks by the flora of the alimentary tract of chickens. *Brit. Poultry Sci.* 14, 627–
570 630.
- 571 Thomas, M.E., Klinkenberg, D., Ejeta, G., Van Knapen, F., Bergwerff, A.A.,
572 Stegeman, J.A., Bouma, A., 2009. Quantification of horizontal transmission of
573 *Salmonella* enterica serovar enteritidis bacteria in pair-housed groups of laying
574 hens. *Appl. Environ. Microb.* 75, 6361–6366.
- 575 Wang, M., Kot, M., 2001. Speeds of invasion in a model with strong or weak allee
576 effects. *Math. Biosci.* 171, 83–97.
- 577 Xiao, Y., Bowers, R.G., Clancy, D., French, N.P., 2005. Understanding the dynamics
578 of *Salmonella* infections in dairy herds: a modelling approach. *J. Theor. Biol.* 233,
579 159–175.

- 580 Xiao, Y., Bowers, R.G., Clancy, D., French, N.P., 2007. Dynamics of infection with
581 multiple transmission mechanisms in unmanaged/managed animal populations.
582 *Theor. Popul. Biol.* 71, 408–423.
- 583 Xiao, Y., Clancy, D., French, N.P., Bowers, R.G., 2006. A semi-stochastic model for
584 *Salmonella* infection in a multi-group herd. *Math. Biosci.* 200, 214–233.
- 585 Zhang-Barber, L., Turner, A.K., Barrow, P.A., 1999. Vaccination for control of
586 *Salmonella* in poultry. *Vaccine* 17, 2538–2545.

Accepted manuscript